Plasma Science and Applications (ICPSA 2013)
International Journal of Modern Physics: Conference Series
Vol. 32 (2014) 1460317 (11 pages)

DOI: 10.1142/S2010194514603172

Plasma focus ion beam- scaling laws

S. H. Saw

INTI International University, 71800 Nilai, Malaysia
Institute for Plasma Focus Studies, 32 Oakpark Drive, Chadstone, 3148 Australia
sorheoh.saw@newinti.edu.my

Published 13 August 2014

Measurements on plasma focus ion beams include various advanced techniques producing a variety of data which has yet to produce benchmark numbers. Recent numerical experiments using an extended version of the Lee Code has produced reference numbers and scaling trends for number and energy fluence of deuteron beams as functions of stored energy E_0. At the pinch exit the ion number fluence (ions m^{-2}) and energy fluence (J m^{-2}) computed as 2.4-7.8×10^{20} and 2.2-33×10^6 respectively were found to be independent of E_0 from 0.4 – 486 kJ. This work was extended to the ion beams for various gases. The results show that, for a given plasma focus, the fluence, flux, ion number and ion current decrease from the lightest to the heaviest gas except for trend-breaking higher values for Ar fluence and flux. The energy fluence, energy flux, power flow and damage factors are relatively constant from H_2 to N_2 but increase for Ne, Ar, Kr and Xe due to radiative cooling and collapse effects. This paper reviews this work and in a concluding section attempts to put the accumulating large amounts of data into the form of a scaling law of beam energy E_{beam} versus storage energy E_0 taking the form for deuteron as: $E_{beam}= 18.2E_0^{1.23}$; where E_{beam} is in J and E_0 is in kJ. It is hoped that the establishment of such scaling laws places on a firm footing the reference quantitative ideas for plasma focus ion beams.

Keywords: Plasma Focus; Plasma Focus Modelling; Plasma Focus Ion Beams.

1. Introduction

A recent survey[1] of ion beam measurements in plasma focus (PF) devices showed a wide range of experimental methods producing results (using mostly inappropriate, even confusing units) which are neither correlated among the various methods and machines nor show any discernible scaling or trend. That paper suggested that since the ion beam exits the focus pinch as a narrow beam with little divergence, the exit beam is best characterized by the yield of ion number per unit cross-section per shot or the fluence per shot. To compute the fluence that paper noted that D-D neutron yield and scaling were already successfully computed by means of a beam-gas target neutron generating mechanism[2-6] in the Lee Model code[7]. Since the deuteron fluence was already implicit in the neutron yield equation, it was a natural step to deduce the deuteron fluence equation, incorporate it in the Lee Model code and hence compute the fluence and other ion beam

properties. This was done for a number of machines. The main results[1] were that: deuteron number fluence (ions m^{-2}) and energy fluence (J m^{-2}) computed as $2.4\text{-}7.8\times10^{20}$ and $2.2\text{-}33\times10^{6}$ respectively were independent of storage energy E_0 from 0.4 – 486 kJ. Typical inductance machines (33-55 nH) produce $1.2\text{-}2\times10^{15}$ ions per kJ carrying 1.3-4 % E_0 at mean ion energy 50-205 keV. Thus that paper defined appropriate ion properties and established reference numbers for these properties for the case of deuterons.

A second paper followed[8] to compute beam ion fluence and flux and other beam properties such as the damage factor in various gases: H_2, D_2, He, N_2, Ne, Ar, Kr and Xe. That study may be useful to assist in the selection of gases for materials application such as damage studies where gases with high ion beam damage factor and power flow may be important; or in materials fabrication where uniformity may require a gas having a lower damage factor whilst having higher values of fast plasma stream energy with a bigger radial distribution.

The PF dynamics is divided into two major phases[9-11]: the axial and the radial. In the axial phase a current sheath is driven down the coaxial channel between the anode and concentric cylindrical cathode in the direction from left to right in Fig1[12]. At the end of the axial phase, the radial phase begins in which a cylindrical current sheath is driven radially inwards, preceded by a shock wave. When the shock wave goes on-axis a stagnated pinch column is formed with the boundary of the stagnated region moving outwards. This boundary may be characterised as a reflected shock wave (RS) separating a radially inward region of doubly shocked gas of higher density and temperature from the outer region of inward streaming plasma driven by the inward moving radial current sheath (piston). When the outwardly moving RS meets the incoming piston the focus pinch phase begins. The radiation from the dense hot pinch plasma may become sufficient to affect the plasma dynamics in terms of radiation cooling and radiation collapse[13] in the case of high Z gases such as Ar, Kr or Xe. From experimental observations it was suggested[14] that Ar (Z=18) is the transition gas in the sense that for gases with Z<18 the pinching proceeds as a column whereas for gases with Z>18 the pinching breaks the column up into a line of densely collapsed hot spots. The dynamics of the current sheath causes large changes of inductance dL/dt and rates of change of current dI/dt. Large electric fields are induced. These and the extreme conditions of the pinch lead to observed plasma disruptions. Besides electromagnetic radiations from the focus, particles are also emitted: generally ion beams axially away from the anode and relativistic electrons (REB) towards the anode. In this paper we focus on the ion beams. We use the mechanism proposed by Gribkov et al[2]. A beam of fast deuteron ions is produced by diode action in a thin layer close to the anode (see Fig 1[12]), with plasma disruptions in the pinch generating the necessary high voltages, terminating the quasi-static nature of the pinch so that its duration is related to the transit time of relevant small disturbances across the pinch column[7].

During the radial compression phase, energy is imparted to the plasma and stored in the increasing inductance of the pinch column. Some of this accumulating energy is emitted as radiation, primarily line radiation in the case of high Z gases and also provided to the ion and REB. The remnant energy may be considered to manifest in the fast plasma stream (FPS).

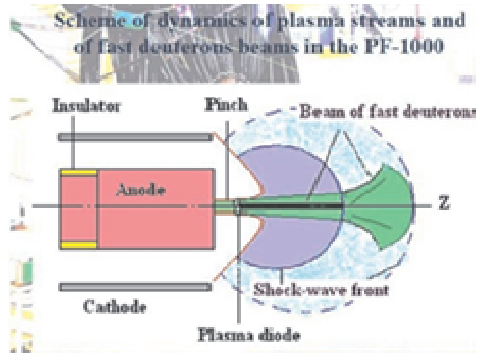

Fig. 1. Schematic12 of the post- pinch FIB (fast ion beam illustrated here with deuterons) and FPS (fast plasma stream) indicated by the post-pinch shock wave.

2. The Method

2.1. *The ion beam flux and fluence equations*

We proceed to estimate the flux of the ion beam. We write the ion beam flux as $J_b=n_b v_b$ n_b=number of beam ions N_b divided by volume of plasma traversed, v_b=effective speed of the beam ions. All quantities are expressed in SI units, except where otherwise stated.

We derive n_b from pinch inductive energy considerations and v_b from the accelerating voltage taken as diode voltage U with this resulting equation:

$$\text{Flux} = J_b = 2.75\times10^{15}\ (f_e/[MZ_{eff}]^{1/2})\{(\ln[b/r_p])/(r_p^2)\}(I_{pinch}^2)/U^{1/2} \quad \text{ions m}^{-2}\text{s}^{-1} \qquad (1)$$

where M=ion mass, Z_{eff}=average effective charge of the ion in the pinch, b=cathode radius, r_p=pinch radius and I_{pinch}=pinch current. The parameter f_e is the fraction of energy converted into beam energy from the inductive energy of the pinch. Analyzing neutron yield data[1,3,4] and pinch dimensional-temporal relationships[15] we estimate f_e=0.14.

In this manner starting from first principles we derived exactly the same equation as we did using empirical formula calibrated at a 0.5MJ point of neutron yield. In this derivation we need only one additional condition: f_e=0.14 and the approximate scaling[15]: $\tau=10^{-6}z_p$. This condition f_e=0.14 is equivalent to ion beam energy of 3%-6% E_0 in the case when the pinch inductive energy holds 20%-40% of E_0. Our extensive study of high performance low inductance PF classified[16] as Type 1 shows that this estimate of f_e is consistent with data. We summarise the assumptions:

(i) Ion beam flux J_b is $n_b v_b$ with units of ions $m^{-2}s^{-1}$,
(ii) Ion beam is produced by diode mechanism[2],
(iii) The beam is produced uniformly across the whole cross-section of the pinch,
(iv) The beam speed is characterized by an average value v_b,
(v) The beam energy is a fraction f_e of the pinch inductive energy, taken as 0.14 in the first instance; to be adjusted as numerical experiments indicate,

(vi) The beam ion energy is derived from the diode voltage U,

(vii) The diode voltage U is $U=3V_{max}$; a relationship obtained from data fitting in extensive earlier numerical experiments[3,4].

The value of the ion flux is deduced in each situation by computing the values of Z_{eff}, r_p, I_{pinch} and U; configuring the Lee Model code with the parameters of the specific machine and gas. The code and the procedure are discussed in more detail in the next section.

2.2. *The Lee Model Code*

The code[7] couples the electrical circuit with PF dynamics, thermodynamics and radiation. It is energy-, charge- and mass- consistent. It was described in 1983[8] and used in the design and interpretation of experiments[9,10,17,18]. An improved 5-phase code incorporating finite small disturbance speed[19], radiation and radiation-coupled dynamics was used[20,21], and was web-published[22] in 2000 and 2005[23]. Plasma self- absorption was included[22] in 2007. It has been used extensively as a complementary facility in several machines, for example: UNU/ICTP PFF[17,18,20,21], NX2[21,24], NX1[21], DENA[25]. It has also been used in other machines for design and interpretation including sub-kJ PF machines[26], FNII[27] and the UBA hard x-ray source[28]. Information computed includes axial and radial dynamics[17] and pinch properties[15], SXR emission characteristics and yield[20,21,24,29-34], design of machines[15,17,21,24,26], optimization of machines[3-6,17,26] and adaptation to Filippov-type DENA[25]. Speed-enhanced PF[10] was facilitated. Plasma Focus neutron calculations[3-6], current and neutron yield limitations[4-6], neutron saturation[5,6], radiative collapse[13], current-stepped PF[35] and extraction of diagnostic data[34-39] and anomalous resistance data[16,40] from current signals have been studied [7]. The code is currently being used to produce reference numbers for ion beams in plasma focus machines operated in various gases[1,8].

2.3. *Procedure used in the numerical experiments*

We use the NX2[21] for these numerical experiments to study the number and energy flux and fluence in various gases including : H_2, D_2, He, N_2, Ne, Ar, Kr and Xe, giving a good range in mass and charge numbers. We configure the NX2 as follows:

- Capacitor bank parameters: L_0=20 nH; C_0=28 μF, r_0=2.3 mΩ,
- Tube parameters: b=4.1 cm; a=1.9 cm, z_0=5 cm,
- Operating parameters: V_0=14 kV; P_0= appropriate range of pressures.

Here L_0=static inductance, C_0=bank capacitance, r_0=short circuited resistance of circuit; b=cathode radius, a=anode radius, z_0=effective anode length; V_0=charging voltage and P_0=operating pressure. A range of pressures ia chosen so that the PF axial run-down time covers a range encompassing 0.5 to to 1.3 of the short-circuit rise time so that the the strongest and also the weakest pinches occur within the selected range. For each shot the dynamics is computed and displayed with ion beam properties. For H_2, D_2, He, N_2 and Ne the procedure is relatively simple even though Ne already exhibits enhanced compression due to radiative cooling.

For Ar, Kr and Xe, the radiation yield (almost wholly the line yield) is severe and radiative collapse has to be adjusted in terms of minimum radius of compression r_{min} (defined by radius ratio r_{min}/a) and time of the pinch; so that the remnant FPS energy remains at least minimally positive. This adjustment involves studying the line yield, the ion beam energy and the FPS energy as well as the value of f_e point by point. The final results contain a degree of uncertainty; each strong radiative collapse point could be adjusted a little differently (by 10% or so) in distribution of energies. However extensive studies show that despite uncertainty of the few strong radiative collapse points the picture of energy distributions is clear and unambiguous.

We point out here that we model the radiative collapse as a whole column whereas experimental observations[14] indicate that Ar is the transition gas below which (lighter gases) the pinch compresses as a column whilst for heavier gases (Kr and Xe) the compression breaks up into a line of hot spots. Our numerical experiments indicate from energy considerations that when the compression breaks up into hot spots the current does not all flow through the hot spots. There is a substantial flow of current in a less compressed column in which the line of hot spots is 'embedded'. The effect of energy transfer and inductance is less severe than indicated by collapse-as-a-column modelling.

3. Results and Discussions

3.1. *Discharge current and general dynamics*

Figure 2(a) shows the PF current computed for the NX2 that is fitted to the measured current to obtain the model parameters f_m, f_c, f_{mr} and f_{cr}[32,33,41]. Figure 2(b) shows the computed radial trajectories of the radially inward shock wave, the reflected radially outward shock wave, the piston trajectory and the pinch length elongation trajectory.

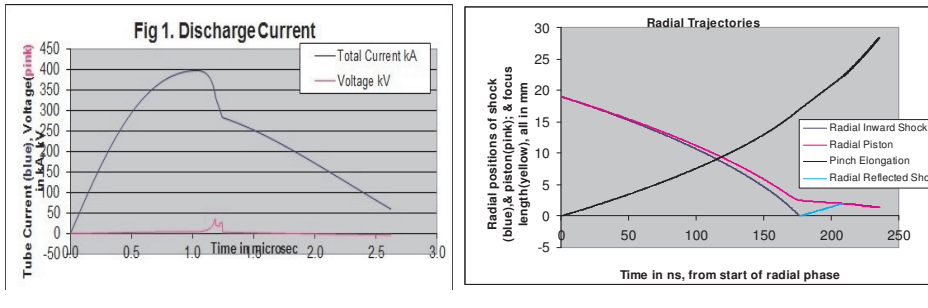

Fig. 2. NX2 Ne 3 Torr (a) Typical discharge current (b) Radial trajectories.

3.2 *Radius ratios for various gases*

The appropriate range of pressures is widest for the lightest gas **H_2,** operated from 1 Torr with 70 Torr still producing a weak pinch. For D_2 and He the range reduces to 1- 40 Torr; for Ne: 0.1 to 10 Torr; for N_2: 0.1 to 6 and for Xe: 0.05-1.8 Torr.

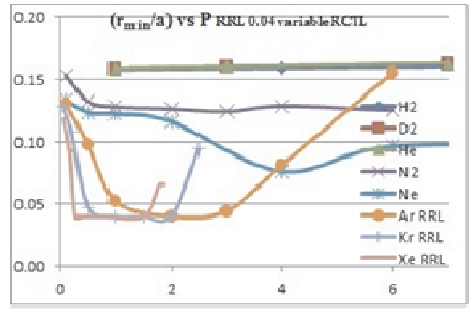

Fig. 3. Radius ratio vs P in Torr for different gases. RRL=radius ratio limited to 0.04; RCTL=radiative cooling time limited to a fraction of the pinch duration.

Figure 3 illustrates the compression of the PF pinch. In H_2, D_2 and He the radius ratio stays above 0.15, the 3 lines staying together up to 10 Torr towards 0.2 for D_2 and He; and 0.18 for H_2. The higher pressures are not shown in Fig 3. For N_2 the radius ratio drops from 0.15 to 0.13 over its useful range of operation. Ne shows signs of enhanced compressions between 3 to 5 Torr indicated by the smaller radius ratio down to a minimum of 0.08 at 4 Torr. Ar shows strong radiative collapse with a radius ratio of 0.04 (a cut-off value designed to make the energy distribution adjustments feasible) over a narrow range of pressure around 2.0 Torr; Kr from 0.5-2 Torr whilst Xe over 0.3 to 1.5 Torr, these latter being a large proportion of their range of operation.

3.2. *Ion beam flux for various gases*

Figure 4a shows the flux in ions m^{-2} s^{-1} for the various gases. The H_2 curve starts at low pressures with a value of $6x10^{27}$ at 1 Torr, rising to peak of 1.9×10^{28} at 25 Torr.

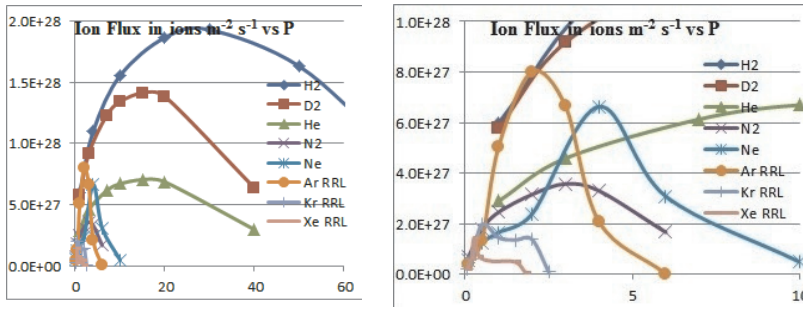

Fig. 4. a) Flux in ions $m^{-2}s^{-1}$ vs Pressure in Torr for various gases, b) Flux, expanded scale (re-calculated, some values more accurate than previously published[8]). RRL and RCTL are defined in the caption of Fig 3.

A detailed study shows that 25 Torr is the pressure where the magnetic piston work is optimised for best ion flux for NX2 in H_2. The flux then drops to 10^{28} at 70 Torr. The D_2 and He curves show the same trend with lower peak flux of 1.4×10^{28} and 7×10^{27} respectively at 15 Torr. N_2 shows the same trend peaking at 3.6×10^{27} at 3 Torr. Ne shows an accentuated peak of 6.6×10^{27} at 4 Torr Fig (4b), corresponding to observed

radiative enhanced compression at 4 Torr (Fig 3). Ar flux undoubtedly displays effect of radiative collapse peaking at a highly accentuated $8x10^{27}$ at 2 Torr. For Kr although the radiative compression is even greater than Ar, the flux is fairly flat at 1.4×10^{27} in the region of 1 Torr; due to the much greater energy per ion of greatly increased mass numbers of 84. The competing effects are more complicated than our first discussion here and will become clearer as we discuss the other properties. Xe shows the same flat flux curve as Kr around 6×10^{26}. Summarising: the beam ion flux drops as the mass number of the ions; with accentuating factors provided by radiatively enhanced compression.

3.3. *Ion beam fluence for various gases*

The shape of the curves and the trend with gases are very similar to the flux; the fluence being the flux multiplied by the ion beam pulse duration. The peak values of the fluence (ions m^{-2}) range from 8×10^{20} for H_2 to 6×10^{18} for Xe; again with clearly radiation-enhanced values of 2×10^{20} and 1.7×10^{20} (ions m^{-2}) for Ar and Ne respectively. The values for each gas are placed in Table 1 for comparison of the main ion beam properties.

3.4. *Beam ion number per kJ*

Figure 5 a-c show that the beam ion number per kJ range from 10^{16} for the lightest gases to 1.5×10^{12} for Xe in the radaitive enhanced regime.

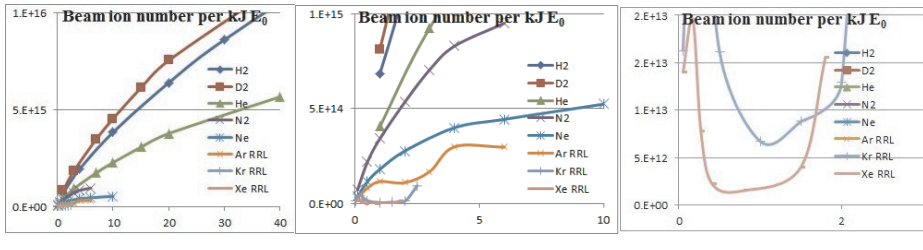

Fig. 5. Beam ion number/kJ as function of P (Torr) in various gases (a) range up to 40 Torr (b) expanded showing up to 10 Torr (c) up to 3 Torr to show Kr and Xe graphs. RRL and RCTL are defined in Fig 3.

3.5. *Beam energy in the various gases*

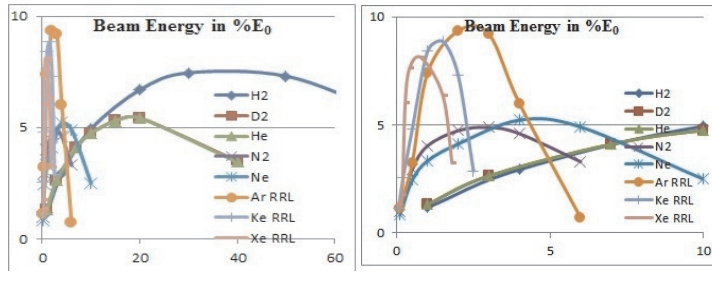

Fig 6. Beam energy as % E_0 versus P (Torr) in various gases. RRL and RCTL are defined in Fig 3.

The results of the numerical experiments show that although the beam ion number is the lowest (see Fig 5) for the heaviest gases Ar Kr and Xe, yet these beams also carry the largest amounts of energy at 8-9% E_0 compared to around 5-8% for the other gases. This is because the energy per ion more than compensate for the low numbers.

3.6. *Damage factor*

The damage factor is defined as power flow density multiplied by (pulse duration)$^{0.5}$. It ranges from the highest value of 2×10^{12} ($Wm^{-2}s^{0.5}$) for Xe to below 10^{10} for the lightest gases. This quantity is considered to be important for assessing the utility of a beam for damage simulation of plasma-facing wall materials in fusion test reactors. (Note: As an approximation, the pulse duration is assumed to be the pinch duration.). The large values of damage factor for Kr and Xe are due to the very large energy per ion for these gases due to radiative collapse.

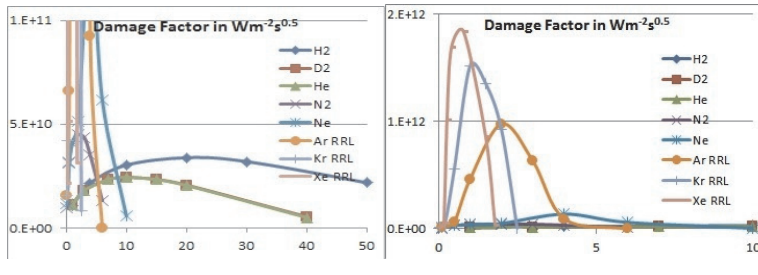

Fig. 7. Damage Factor (a) showing the lighter gases (b) the heavier gases.). RRL and RCTL are defined in the caption of Fig 3.

3.7. *Tabulation of ion beam properties in various gases for comparison*

The above results and some others are tabulated for comparison in Table 1.

Table 1: NX2 Properties and computed Ion beam characteristics (some values have been re-calculated and are more accurate than previously published[8] values.)

NX2	**H2**	**D2**	**He**	**N2**	**Ne**	**Ar**	**Kr**	**Xe**
Pressure (Torr) matched	30	15	15	2	3	2	0.5	0.41
I_{peak} (kA)	397	397	397	395	382	406	390	394
z_p (cm)	2.8	2.8	2.8	2.8	2.8	3.0	2.4	2.3
r_p (cm)	0.33	0.32	0.31	0.24	0.22	0.08	0.08	0.08
τ (ns)	37	37	37	26	21	21	9	5
Z_{eff}	1	1	2	6.4	8.5	11.5	24	28
Ion Fluence ($x10^{20}$ m^{-2})	**7.0**	**5.2**	**2.6**	**0.8**	**0.8**	**1.7**	**0.15**	**0.03**
Ion Flux ($x10^{27}m^{-2}s^{-1}$)	19	14	7	3.2	5.0	8.0	1.9	0.7
Mean ion energy (keV)	54	54	108	553	927	5250	18601	215664
FIB Energy (%E_0)	7.5	5.3	5.3	4.7	4.1	9.3	4.8	7.6
Dam Fr ($x10^{10}Wm^{-2}s^{0.5}$)	**3.2**	**2.3**	**2.3**	**4.5**	**5.1**	**98**	**55**	**170**
Ion Number/kJ ($x10^{14}$)	86	61	31	5.3	2.8	1.1	0.16	0.02

4. Conclusion

In this paper we reviewed the flux equation of ion beams in PF for any gas. The flux equation is incorporated into the code and the number and energy flux and fluence from different gases are computed for NX2. The results portray the properties of the ion beam at the pinch exit. The ion fluence ranges from 7×10^{20} (m^{-2}) for H_2, decreases through the heavier gases to 1.7×10^{20} for Ar and more dramatically to 0.03×10^{20} for Xe. The very small fluence value of Xe is due to the very large energy of the Xe ion, with average Z_{eff} of 28 and accelerated by large electric fields induced in the radiative collapse.

The ion number goes from 86×10^{14} per kJ for H_2, decreases to 2.8×10^{14} per kJ for Ne and then to 0.02×10^{14} for Xe. The beam energy drops slightly from 7.5 % of E_0 for H_2 to 4.1% of E_0 for Ne and then increases to 9% for Ar and 7.6 % for Xe. The damage factor is highest for Xe at 170×10^{10} $Wm^{-2}s^{0.5}$ dropping to about 100×10^{10} for Ar and to $2\text{-}5\times10^{10}$ for the lighter gases. The results for Kr and Xe and to a lesser extent in Ar are very much affected by the way the radiative collapse is modeled; whilst those from H_2 to Ne are not affected by radiative collapse. Overall one might express the opinion that for damage studies, Ar might be the best compromise candidate gas, having a good damage factor, good beam energy and the best beam ion number amongst the 3 heaviest gases.

As a concluding note: we are carrying out many series of numerical experiments on machines from sub-kJ to 1 MJ. A main objective is to obtain and efficiently present relevant scaling laws. One of the first results we have obtained (for PF deuteron beams) is presented in Fig 8. This is an attempt to put ion beam reference numbers on the same footing as neon soft x-ray yield Y_{sxr} (Y_{sxr} scaling law has been obtained in numerical experiments[42] whilst it is well-known that neutron scaling law is firmly established[2,3,5,6]).

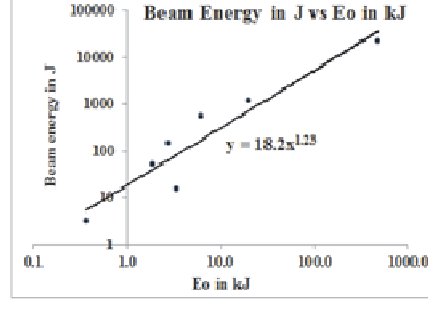

Fig. 8. Establishing a first scaling law for deuteron beam energy.

From Fig 8: $E_{beam}(J) = 18.2E_0^{1.23}$ (E_0 in kJ). We note the considerable scatter with square of residual 'R^2' of 0.89, deviating considerably from the perfect value of 1.00.

We emphasize that this is a first attempt that needs to be confirmed with more numerical experiments and with laboratory measurements, in order to put quantitative ideas of ion beams on a firm footing.

Acknowledgments

This work is partially supported within IAEA Research Contract: 16934 of CRP F1.30.13 (Investigations of Materials under High Repetition and Intense Fusion-relevant Pulses). The author also acknowledges research grants INT-CPR-01-02-2012 and FRGS/2/2013/SG02/INTI/01/1.

References

1. S Lee and S H Saw, *Phys. Plasmas* **19**, 112703 (2012).
2. V A Gribkov et al, *J. Phys. D: Appl. Phys*. **40**, 3592 (2007).
3. S Lee and S H Saw, *J Fusion Energy* **27**, 292 (2008).
4. S. Lee and S H Saw, *Appl. Phys. Lett.* **92**, 021503 (2008).
5. S Lee. *Plasma Physics Controlled Fusion* **50**, 10500 (2008).
6. S Lee. *Appl. Phys. Lett.* **95**, 151503 (2009).
7. S Lee, Radiative Dense Plasma Focus Computation Package: **RADPF.** http://www.plasmafocus.net; http://www.intimal.edu.my/school/fas/UFLF/(archival websites)
8. S Lee and S H Saw, *Phys Plasmas* **20**, 062702 (2013).
9. T.Y.Tou, S.Lee & K.H.Kwek. *IEEE Trans Plasma Sci* **17**, 311 (1989).
10. A Serban and S Lee, *Plasma Sources Sci and Tehnology*, **6**, 78 (1997).
11. S H Saw, P C K Lee, R S Rawat, S Lee, *IEEE Trans Plasma Sci*, **37**, 1276 (2009).
12. V A Gribkov, Presentation at IAEA. Dec (2012).
13. S Lee, S. H. Saw and Jalil Ali, *JOFE* **32**, 42 (2013).
14. F N Beg et al, *J Appl Phys* **88**, 3225 (2000).
15. S Lee & A Serban, *IEEE Trans Plasma Sci* **24**, 1101 (1996).
16. S Lee, S H Saw, A E Abdou and H Torreblanca, *J Fusion Energy* **30**, 277 (2011).
17. S Lee et al, *Amer J Phys* **56**, 62 (1988).
18. SP Moo, CK Chakrabarty, S Lee - *IEEE Trans Plasma Sci* **19**, 515 (1991).
19. D E Potter, Phys Fluids **14**, 1911 (1971).
20. M H Liu, X P Feng, SV Springham & S Lee, *IEEE Trans Plasma Sci*. **26**, 135 (1998).
21. S Lee et al, *IEEE Trans Plasma Sci*, **26**, 1119 (1998).
22. S.Lee in http://ckplee.home.nie.edu.sg/plasmaphysics/ (2012).
23. S. Lee in ICTP Open Access Archive: http://eprints.ictp.it/85/ (2005).
24. D.Wong et al, *Plasma Sources, Sci & Tech* **16**, 116 (2007).
25. V. Siahpoush, M.A.Tafreshi, S. Sobhanian, & S. Khorram, *Plasma Phys Control Fusion* **47**, 1065 (2005).
26. L. Soto et al, *Brazilian J Phys* **34**, 1814 (2004).
27. H.Acuna, F.Castillo, J.Herrera & A.Postal,(*Int conf Plasma Sci*, June 1996), pp. 127
28. C.Moreno, V.Raspa, L.Sigaut & R.Vieytes, *Applied Phys Letters* **89**, 091502(2006).
29. S. Lee, R S Rawat, P Lee and S H Saw, *J. Appl. Phys.* **106**, 023309 (2009).
30. S. H. Saw and S. Lee, *Energy and Power Engineering* **2**, 65 (2010).
31. M. Akel, Sh Al-Hawat, S H Saw and S Lee, *J Fusion Energy* **29**, 223 (2010).
32. Sh. Al-Hawat, M. Akel, S H Saw, S Lee, *J Fusion Energy* **31**, 13 (2012).
33. M.Akel, S.Lee, S.H.Saw, *IEEE Trans Plasma Sci* **40,** 3290 (2012).
34. S Lee et al, *IEEE Trans Plasma Sci* **39**, 3196 (2011).
35. S Lee and S H Saw, *J Fusion Energy* **31**, 603 (2012).

36. S Lee, S H Saw, P C K Lee, R S Rawat and H Schmidt, *Appl. Phys. Lett.* **92**, 111501 (2008)
37. S H Saw et al, *Rev Sci Instruments* **81**, 053505 (2010).
38. S Lee et al, *J Fusion Energy* **31**, 198 (2012).
39. S. Lee, S.H. Saw, L. Soto, S V Springham, S P Moo, *Plasma Phys Control Fusion*, **51** 075006 (2009).
40. R A Behbahani, F M Aghamir, *Phys. Plasmas* **18**, 103302 (2011).
41. S.P. Chow, S. Lee and B.C. Tan, *J Plasma Phys* **8**, 21(1972).
42. S Lee, S H Saw, P Lee, R S Rawat, *Plasma Phys Control Fusion*, **51**, 105013 (2009).